



Cite this: *Environ. Sci.: Nano*, 2017, 4, 886

Tungsten carbide nanoparticles in simulated surface water with natural organic matter: dissolution, agglomeration, sedimentation and interaction with *Daphnia magna*

Jonas Hedberg,^{*a} Mikael T. Ekvall,^b Lars-Anders Hansson,^c Tommy Cedervall^b and Inger Odnevall Wallinder^a

Even though anthropogenic nano-sized tungsten carbide nanoparticles (WC NPs) have been found in the environment, there are currently no investigations on their environmental fate. This work studies the interaction between natural organic matter (NOM) and WC NPs, as well as the potential uptake by the aquatic model organism *Daphnia magna*. We here show that the affinity between WC NPs and humic acid or dihydroxybenzoic acid (DHBA), which are model molecules of NOM, is very low with no observed surface adsorption. The lack of a stabilizing effect of these organic molecules, in combination with a relatively high effective density of WC NP agglomerates in humic acid, resulted in the substantial agglomeration and sedimentation of the WC NPs. A higher stability of the smaller sized WC NP agglomerates (<150 nm) means that this fraction is mobile and can be transported to other settings, suggesting that this particle fraction should be considered in further studies. The dissolution of tungsten from WC NPs was continuous and the relatively slow dissolution rate (on the order of 0.03 mg m⁻² h⁻¹) implies that particle transport will not be severely limited from a dissolution perspective. Uptake of tungsten (dissolved tungsten and WC particles) by *D. magna* was observed although this did not induce any acute toxic effects.

Received 7th December 2016,
Accepted 7th February 2017

DOI: 10.1039/c6en00645k

rsc.li/es-nano

Environmental significance

There are currently no investigations on the environmental fate or potential hazards of nano-sized tungsten carbide particles (WC NPs), even though they have been observed in the environment. Since nanoparticles may give rise to higher toxicity than *e.g.* their dissolved form, the evaluation of WC NPs in the environment is necessary. The key findings are the weak interaction between WC NPs and natural organic matter and the lack of acute toxicity for *Daphnia magna* exposed to WC NPs. These results show that there is likely no reason to be immediately alarmed by the dispersion of WC NPs into the environment. However, further investigations on the smallest particle fraction (<100 nm) and the chronic effects of WC NPs are needed.

Introduction

Tungsten carbide (WC) is used in several applications, including cutting and drilling tools, studded tires, and bullets.¹ Nanoscale WC is deliberately used in for example catalysis,^{2,3} coatings,⁴ and sensors.⁵ These uses of WC cause the dispersion of tungsten into the environment,⁶ and tungsten has for example been detected in the vicinity of military facilities.⁷ In addition, small sized WC particles have been detected in

street dust (size range of 0.1–1.4 μm),⁸ in particles sized <1 μm in roadside snowpacks,⁹ and in the nano-sized fraction (PM_{0.1}) in air in road tunnels.¹⁰ The WC particles in street dust have been attributed to the wear of studded tires and have *e.g.* resulted in a higher content of tungsten in degraded organic matter (humus) under urban conditions compared with that under rural conditions.¹¹

The toxicity of tungsten is in general considered to be low,¹² with *e.g.* a reported EC50 value of 89.4 mg L⁻¹ for W⁶⁺ for *Daphnia magna*.¹³ There are however some forms of tungsten that are more potent, *e.g.* polymerized tungsten.¹⁴ Tungsten alloys have shown to affect soil respiration when present at high enough concentrations.² Nano-sized WC has not been seen to induce acute cytotoxicity in human pulmonary cells, rat neuronal and glial cells or human skin but has been linked to oxidative stress.⁸

^a Dept. Chemistry, Div. Surface and Corrosion Science, KTH Royal Institute of Technology, Drottning Kristinas väg 51, SE-100 44 Stockholm, Sweden.

E-mail: jhed@kth.se

^b Center for Molecular Protein Science, Department of Biochemistry and Structural Biology, Lund University, P.O. Box 118, SE-221 00 Lund, Sweden

^c Aquatic Ecology, Department of Biology, Lund University, Ecology Building, SE-223 62 Lund, Sweden



No studies on the interaction between tungsten and natural organic matter (NOM) are reported in the scientific literature.¹ NOM has been shown in studies of other metal NPs to play an important role as a moderator of particle stability.¹⁵ The lack of data on WC NP–NOM interactions, including stability in terms of agglomeration and transformation/dissolution, hinders the prediction of their environmental fate and the assessment of their potential environmental risks upon dispersion. Hence, the question still remains if nanoscale WC can constitute a risk,¹² e.g. for aquatic organisms, since water from e.g. roads is flushed into lakes and ponds. This warrants further studies on the environmental dispersion of nano-sized WC.

This study aims to give insights into the environmental fate of WC NPs by considering their transformation/dissolution in environmentally relevant matrices, as well as their potential interaction with *D. magna* from a natural food chain perspective. Our studies mimic the initial stages of an exposure scenario where WC NPs are released from e.g. studded tires and dispersed into an aquatic setting. The approach can thus be seen as a first step towards assessing the risks of dispersed WC NPs. *Daphnia magna* is an important species as it serves as fodder for e.g. fish, which may cause effects in the food chain due to bioaccumulation if the NPs are taken up by *D. magna*.¹⁶ There are presently no reports on the uptake of WC NPs, and in order to address this knowledge gap, we investigated the acute toxicity induced by WC on *D. magna* and quantified the uptake of WC NPs. For other nanomaterials such as silver and titanium dioxide, the uptake has been shown to be significant.^{17,18} The interaction between WC NPs and synthetic surface water with dihydroxybenzoic acid (DHBA), a model molecule for small organic degradation products,¹⁹ or humic acid was investigated. Measurements were performed to deduce the size of particle agglomerates, the extent of sedimentation, the surface characteristics, and the release of tungsten. The effective density of the WC agglomerates was determined to gain insights into their transport properties.

Materials and methods

Simulated surface water solutions

Simulated surface water (SW), containing 0.0065 g L⁻¹ NaHCO₃, 0.00058 g L⁻¹ KCl, 0.0294 g L⁻¹ CaCl₂·2H₂O, and 0.0123 g L⁻¹ MgSO₄·7H₂O, adjusted to pH 6.2 ± 0.2 with 5 vol% HNO₃ or NaOH, was used. This pH adjustment added ca. 2 μM of ionic strength, which added only <0.1% in the ionic strength of the studied solutions. The solvent was ultrapure water (18.2 MΩ cm resistivity, Millipore, Solna, Sweden) and all chemicals were of analytical grade (p.a.) or puriss. p.a. grade (in the cases of 65 vol% HNO₃ used to acidify the samples prior to atomic absorption spectroscopy, of 30 vol% H₂O₂ and of 30 vol% NaOH, used for digestion of the W-containing samples). In addition, 2,3-dihydroxybenzoic acid (0.1 mM) in surface water, denoted SW + 2,3-DHBA, and SW containing 3,4-dihydroxybenzoic acid (0.1 mM), denoted

SW + 3,4-DHBA, were used. 2,3-DHBA (99%, Lot # 09705EBV) and 3,4-DHBA (≥97.0% (T), Lot # BCBP0053V) were purchased from Sigma Aldrich, Sweden. The DHBA solutions in SW were prepared 24 h before usage, to ensure the complete dissolution of the DHBA. Humic acid was obtained from the International Humic Substances Society (Suwannee River, humic acid standard II, 2S10H1) and used at a concentration of 20 mg L⁻¹. This concentration of organic matter is within the range of that found in natural waters.²⁰ Humic acid was prepared by dissolving it in 1 mL of 0.1 M NaOH, followed by vigorous stirring. This solution was then diluted in SW and checked with Dynamic Light Scattering (DLS) to ensure the complete dissolution of humic acid.

All pieces of equipment (vials, flasks, tubes, etc.) in contact with the solutions were acid-cleaned in 10 vol% HNO₃ for at least 24 h and rinsed at least four times with ultrapure water.

Nanoparticle dispersion

WC NPs were purchased from American Elements, Los Angeles, CA, USA (<100 nm, W-C-03M-NP.100N, Lot # 1221393479-611, 99.9% metal basis purity).

Sonication was performed using a probe sonicator (Branson Sonifier 250, Ø 13 mm, 400 W output power, 20 kHz). The calibration of the acoustic energy delivered during sonication was based on the established protocols for NP dispersion.²¹ It involves a calorimetric method to calibrate the delivered acoustic energy by adjusting the probe sonicator amplitude. For the probe used in this study, a 20% sonication amplitude (continuous mode) for 180 s was used. These settings correspond to a delivered acoustic energy of 1440 J. See more details elsewhere.²² NPs with concentrations of 1 g L⁻¹ were sonicated for 180 s in ultrapure water in Scint-Burk vials (WHEA986581, Wheaton Industries Inc., USA). The glass vials were positioned in an ice-filled bowl with the sonication probe inserted between the upper quarter and the upper half of the solution in the vial. NP dispersions from these stock solutions were then diluted to reach a final particle concentration of 0.1 g L⁻¹ and used directly after the dispersion.

Sedimentation rate and metal release investigations

6 ± 0.2 mg of WC NPs was introduced into an acid-cleaned glass vial. 6 mL of MilliQ water was added to the vials (stock solution, 1 g L⁻¹ NPs) and the NPs were dispersed using sonication as described above. 1.5 mL of the sonicated stock solution was pipetted to an acid-cleaned 60 mL PMP Nalgene® jar and diluted with the solution to a final concentration of 0.1 g L⁻¹ NP (total volume of 15 mL). This was repeated twice, generating three replicates. A blank sample without any NPs was prepared in parallel. The replicates and the blank sample were incubated at 25 °C (bilinear shaking at 22 cycles per min, 12° inclination, Platform-rocker incubator SI80, Stuart) for 1, 2, 4, 6, 24, and 528 h (22 days). A new stock solution was freshly prepared just before the start of exposure. After incubation, 5 mL of each replicate was pipetted to an acid-



cleaned plastic tube and another 5 mL was filtered through an inorganic membrane filter (0.02 μm , 25 mm diameter, alumina, Anotop 25 syringe filter, GE Healthcare Life Sciences) to an acid-cleaned plastic tube. The samples were diluted with a 5 mL 50/50 mixture of 0.2 wt% NaOH/30 vol% H_2O_2 , sonicated in a sonication bath for 1 h (at 25 $^\circ\text{C}$), and stored for at least 4 days at room temperature prior to solution analysis. This digestion procedure was sufficient for complete particle dissolution, with a mean recovery of 89%, ranging from 82 to 98%.

In addition, three dose tests (triplicates) were prepared from every stock solution directly after sonication in order to determine the actual dose for each exposure, as the real dose can be lower than the nominal dose due to sedimentation.²² 3×0.25 mL was pipetted from each stock solution after sonication and digested as described above.

Validation of sample preparation and digestion procedures

Since ultracentrifugation was found to be insufficient for solid–liquid separation of particle suspensions, an inorganic 0.02 μm membrane filter was used. In order to estimate the potentially induced errors due to either contamination from or adsorption of metal ions on the membrane, solutions of different known ion concentrations of W (from Perkin Elmer W standard) were prepared and filtered. Both filtered and non-filtered samples were analyzed for the total W concentration, showing some adsorption of W on the filter (<10%).

Metal analysis in solution

Determination of W was performed using inductively coupled plasma atomic emission spectroscopy (ICP-AES, Thermo Scientific iCAP 6000 series ICP spectrometer). Standards were prepared in 0.1 vol% NaOH and calibration was based on a blank value of zero (0.1 vol% NaOH) and at least three calibration standards covering the sample concentration range (10–100 $\mu\text{g L}^{-1}$ for *D. magna* and 0.5–30 mg L^{-1} for W release). Quality control samples of known concentrations were analyzed approximately every 10th sample and did not deviate more than 10% from their nominal value. The detection limit was estimated to be 5 $\mu\text{g L}^{-1}$, three times the standard deviation of the blank samples. The limit of determination was approx. 17 $\mu\text{g L}^{-1}$ (ten times the standard deviation).

Particle size measurements by means of photon cross correlation spectroscopy

A stock solution was prepared as described above. After diluting the stock solution to a NP concentration of 0.1 g L^{-1} , 1 mL of the solution was added to a cuvette (Eppendorf AG, Germany, UVette Routine pack, Lot # C153896Q). This was repeated twice, generating three replicates. The replicates were analyzed by photon cross-correlation spectroscopy (PCCS) using a Nanophox instrument (Sympatec GmbH, Clausthal, Germany). The samples were incubated at 25 $^\circ\text{C}$ (Cultura mini-incubator 13311, Merck) between the measurements.

Before initiation of the first measurement, the instrument was put on standby for 2 min in order to let the temperature of the replicates be 25 $^\circ\text{C}$. A latex standard was tested prior to analysis in order to ensure the accuracy of the instrument. The algorithm used to obtain the mass size distribution was the non-negative least squares (NNLS) analysis. The results are presented as d_{50} values obtained from the intensity size distribution measurements.

Zeta potential measurements

The electrophoretic mobility of the NPs was measured using a Malvern Zetasizer Nano Z instrument. The NPs were first dispersed in an ultrasonic bath for at least 3 min and then transferred using a syringe to Malvern Zetasizer Nanoseries cuvettes, avoiding the rapid sedimentation of the particle fraction. The Smoluchowski approximation was used to calculate the zeta potential from the electrophoretic mobility. The electrophoretic mobility was measured in triplicate readings for each sample.

Transmission electron microscopy

Transmission electron microscopy (TEM) investigations were performed using a Hitachi HT7700 microscope, operating at 100 kV. Samples were prepared by dispersing the particles in butyl alcohol at a concentration of 1 g L^{-1} and sonicated as described above. The suspensions were then pipetted onto TEM copper grids coated with holey carbon films (Ted Pella) from which the solvent evaporated under ambient laboratory conditions (20 $^\circ\text{C}$). TEM images were recorded in bright field mode.

Nitrogen absorption measurements

The surface area to weight ratio (specific surface area) of each powder was determined by means of the Brunauer–Emmett–Teller method²³ (Micromeritics GEMINI V) that measures the adsorbed amount of nitrogen under cryogenic conditions.

X-ray photoelectron spectroscopy

With X-ray photoelectron spectroscopy (XPS) using a Kratos AXIS UltraDLD X-ray photoelectron spectrometer (Kratos Analytical, Manchester, UK) driven by a monochromatic 150 W Al X-ray source, the outermost (5–10 nm) surface of the NPs was investigated (analysed areas approximately sized 700 \times 300 μm). Detailed spectra were obtained for C 1s, O 1s and W 4f. The NPs were mounted on copper tape, which did not contribute to the signal, to fix them against the diffusion in the applied vacuum inside the ultra-high vacuum instrumental chamber. All binding energies were corrected to the C 1s contamination peak at 285.0 eV.

Attenuated total reflection Fourier transform infrared spectroscopy

A Bruker Tensor 37 FTIR spectrometer was used together with a Platinum ATR-IR accessory. The ATR-IR spectroscopy



was equipped with a diamond crystal and the angle of incidence of the IR beam was 45°. The spectra were collected at 4 cm⁻¹ resolution and 256 scans were co-added for each spectrum.

The WC NPs were dispersed as described above, with the difference being that the medium was ethanol and that the particle loading was 2.5 g L⁻¹ in the sonicated stock solution. This dispersion was drop cast onto the ATR crystal. The total deposited volume was *ca.* 50 µL. The film was left for 2 h before measurement. After that, an ATR-IR flow accessory was put onto the film and surface water was used to rinse the system to remove any loosely attached NPs. A spectrum of the particle film and surface water was used as the background for the studied NP solutions of interest. Control experiments confirmed the lack of contribution from the bulk species in the absorption spectra of the WC NPs.

Volumetric centrifugal method (VCM)

NP dispersions were prepared as described in the section on Nanoparticle dispersion above. After that, 0.1 mL of the dispersion was added to 0.9 mL of 20 mg L⁻¹ humic acid at pH 6.2 in a PVC cell culture tube (TPP, Switzerland, Lot # 20090063). Three replicates and one blank were prepared. The cuvettes were then centrifuged for 1 h at 3000g (Centrifuge 5702, Eppendorf). The volume of the pellet was determined using a sliding ruler equipped with a magnifying glass device from TPP (product no. 87010). The effective density of the WC agglomerates was determined to be 2.4 ± 0.3 g cm⁻³, as deduced from a pellet volume of 0.09 ± 0.02 µL. See more details of the VCM elsewhere for calculating the effective density.²⁴ The bulk density of WC (15.63 g cm⁻³) was used in the calculation. The assumed packing factor was set to 0.634, which corresponds to randomly packed spheres.²⁵

Sedimentation velocity calculations

Predictions of the NP sedimentation velocity were mainly based on the work of Hinderliter *et al.*,²⁶ using the Matlab program for ISDD modelling obtained from the same study. The *In vitro* Sedimentation, Diffusion, and Dosimetry model (ISDD) is a computational model for diffusion, sedimentation, and dosimetry. It is based on the sedimentation and diffusion of spherical NPs and uses Stokes' law and the Stokes-Einstein equation. Advection is not considered. To simulate sedimentation of NPs, the ISDD model solves the resulting partial differential equation in the vertical dimension.

Daphnia magna toxicity and uptake

In order to evaluate the toxicological effect of the WC NPs from a food chain perspective, we first exposed algae (*Scenedesmus* sp.) to WC NP concentrations ranging from 100 mg L⁻¹ to 0.001 mg L⁻¹. The WC NPs were dispersed using ultra-sonication for 10 min in 50/50 pulse mode (Heat Systems model CL4, Heat Systems). The concentrated dispersion was added to an algal suspension and the solution was mixed for two minutes and left to stand

for 24 h. A control treatment containing only water and algae was used as reference. After 24 h, the solutions were mixed again and ten *D. magna*, originating from a laboratory culture collected in Lake Bysjön (southern Sweden), were introduced into each tube where they could feed on the algae for 24 h. Thereafter, the number of surviving individuals was recorded in each tube. Each treatment was replicated three times and the data were analyzed by one-way ANOVA using GraphPad Prism (version 6.0h). A set of replicates (*i.e.* one control + WC NP treatments) was rerun if the mortality in the control exceeded 20%.

To quantify the uptake of WC by *D. magna*, 15 *D. magna* were exposed to algal suspensions containing WC NPs with concentrations of 10 and 0.1 mg L⁻¹, as described above. A control treatment containing only water and algae was used as reference. After 24 h of feeding on the algal suspension, all individuals were isolated from each treatment using a small mesh filter (mesh size ~250 µm) and rinsed with MilliQ water. After rinsing, each individual animal was measured using a stereo microscope (Olympus SZX7), placed in individual tubes, frozen at -80 °C and freeze dried for 24 h. The individual animals were digested in 1.5 mL of H₂O₂, 1.5 mL of 0.2% NaOH and 3 mL of MilliQ water using a Metrohm 705 UV Digester for 15 min. Thereafter, the tungsten was dissolved and analyzed according to the method described above. This whole procedure resulted in a recovery of >90% for added WC NPs in control experiments. All measured concentrations were normalized to animal dry mass according to the length-weight relationships described by Dumont *et al.*²⁷ and Bottrell *et al.*²⁸ Measurements that fell below the detection limit of 0.03 µg per mg dry weight of *D. magna* were all set equal to the detection limit (*i.e.* 0.03) to enable analysis of the data. The detection limit for the uptake was based on the detection limit of ICP (5 µg L⁻¹). Differences in the uptake were analyzed by one-way ANOVA using GraphPad Prism (version 6.0h).

Joint expert speciation system

Joint expert speciation system (JESS, v. 3.0) software²⁹ was used to estimate the speciation of soluble W in SW and DHBA. Humic acids are not available in the JESS software. In addition to the respective solution compositions, other input values were a temperature of 25 °C and a redox potential of 285 mV. The redox potential was measured in the solutions of interest using an InLab Redox ORP electrode, calibrated with an ORP standard solution according to the manufacturer's instructions (Mettler Toledo).

Results and discussion

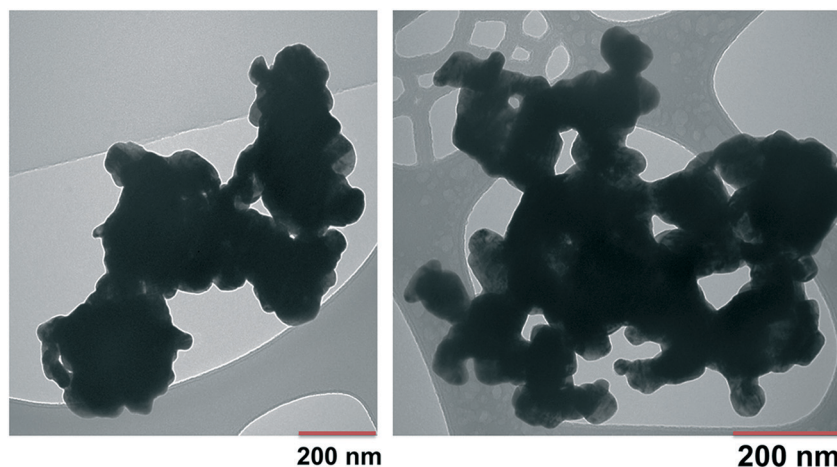
Characteristics of the studied WC NPs

Particle and surface characteristics of the WC NPs are given in Table 1 and the TEM pictures show the primary particle sizes varying between 20 and 200 nm (Fig. 1). The exact isoelectric point of WC could not be determined as it was very



Table 1 Characteristics of WC NPs

| | |
|--|---|
| Primary size (nm), TEM | 20–200 |
| Zeta potential (mV), pH 6.2, in surface water | -21 ± 5 |
| Isoelectric point (pH) | < 2 |
| Surface compounds, XPS | WO_3 , $\text{WO}_2 + \text{W}(\text{vi})$, $\text{W}(\text{vi})$ suboxides |
| Specific surface area ($\text{m}^2 \text{g}^{-1}$), BET | 1.76 |
| Effective density (g cm^{-3}), in 20 mg L^{-1} humic acid, pH 6.2 | 2.4 ± 0.3 |

**Fig. 1** TEM pictures of WC NPs. Images were obtained in bright field mode.

low ($< \text{pH } 2$), which illustrates the acidic nature of the oxides formed on the WC NPs. The outermost surface of the unexposed WC NPs was highly oxidized, judging from the XPS findings. The main surface components were WO_3 and WO_2 as well as other oxidized tungsten (iv and vi) compounds. Additional information is given elsewhere.³⁰

Agglomeration, dissolution, sedimentation, and surface characteristics of WC NPs in surface water

The size of the agglomerates (d_{50} values) decreased over time for both SW and SW + 20 mg L^{-1} humic acid, as shown in Fig. 2A. Fig. 2B depicts the sedimentation of WC NPs in SW,

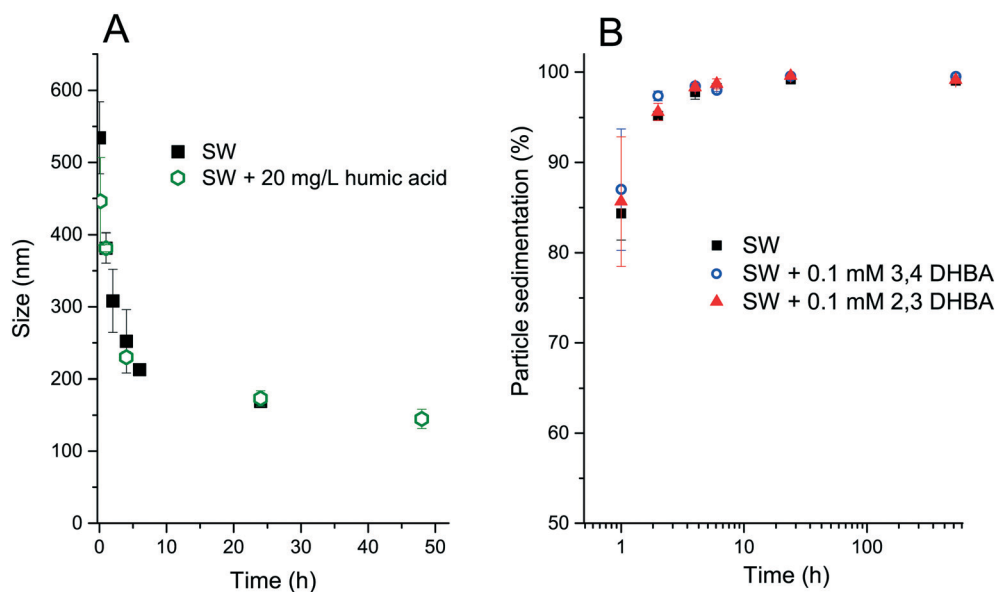


Fig. 2 A: Agglomerate size (d_{50}) as a function of time for 0.1 g L^{-1} WC NPs exposed to SW and SW + 20 mg L^{-1} humic acid at pH 6.2. B: Fraction of sedimented WC NPs as a function of time (note: log-axis) for 0.1 g L^{-1} WC NPs exposed to SW, SW + 0.1 mM 3,4-DHBA, and SW + 0.1 mM 2,3-DHBA. All error bars represent one standard deviation as calculated from three individual replicate measurements.



SW + 0.1 mM 2,3-DHBA, and SW + 0.1 mM 3,4-DHBA. The results show that >99 wt% of the WC NPs sediment within 10 h, as investigated in a container with a 10 mm media height.

The sonication procedure was not capable of totally dispersing the WC NP powder as seen from the initial presence of large-sized agglomerates. Extensive agglomeration is expected for non-functionalized metal NPs with moderately low zeta potentials (approx. |20| mV) due to the strong attractive van der Waals forces between the NPs.²² The reduction in the size of the agglomerates over time indicates sedimentation of the larger-sized agglomerates, leaving the smaller-sized particles in the solution.

Fig. 3 shows theoretical estimates of the sedimentation rates of WC NPs using the ISDD model. The modelling used the measured effective density ($2.4 \pm 0.3 \text{ g cm}^{-3}$) of the WC agglomerates in 20 mg L^{-1} humic acid at pH 6.2. The measured effective density was significantly smaller than the bulk density of WC (15.63 g cm^{-3}), due to the porosity and fractal nature of the agglomerates.²⁶ Its value was in the same order, although somewhat higher, compared to those obtained from measurements of other metal NPs in biological media.³¹ The results in Fig. 3 are qualitatively in line with the reduction in size with time as seen for the WC agglomerates in Fig. 2B. The sedimentation velocity for the 150 nm sized agglomerates was significantly reduced (approx. 10 times) compared with the 500 nm sized agglomerates. By assuming 500 nm sized agglomerates, the calculated sedimentation rate in Fig. 3 is almost a factor of two lower than the observed rates in Fig. 2B. This underestimation of the calculated sedimentation rate could be related to the fact that the flow of water through the agglomerates is not considered in the ISDD calculations.³² Also, the presence of <500 nm sized agglomerates (Fig. 2) will influence the comparison.

The data in Fig. 2 and 3 imply that the transport of the larger sized WC particles will be very limited and that the smaller sized particles and agglomerates (<150 nm) are more mobile and have the potential for further transport to other settings. This is however only true if homoagglomeration is

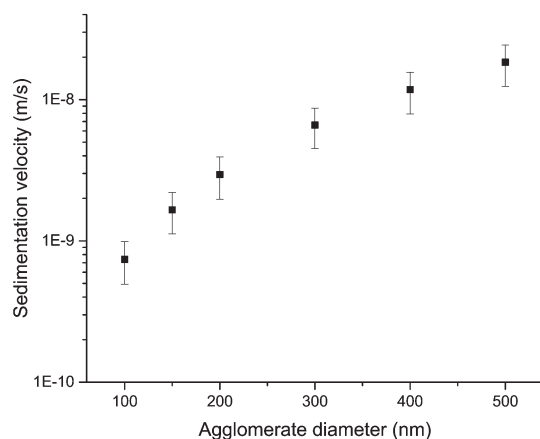


Fig. 3 Sedimentation velocities as a function of particle agglomerate size, as calculated using the ISDD model.

considered. The possibility of the formation of hetero-agglomerates, which is often an important factor for NP transport,^{33,34} still needs to be investigated. For example, Peltola *et al.* found WC attached to mineral grains in street dust.⁸ A factor that can counteract the transport is the retention of tungsten by soil and minerals.²

No stabilizing effect of either DHBA or humic acid was observed on the WC NPs, as seen from the results in Fig. 2. Moreover, the ATR-IR data showed no peaks corresponding to the adsorption of the functional groups of DHBA or humic acid (Fig. 4). To our knowledge, no literature studies that investigate the surface interactions between WC particles and organic molecules relevant to natural waters exist. WO_3 , which is present on the WC NP surface (Table 1), has under vacuum been seen to molecularly adsorb alcohols, with dissociation taking place at higher temperatures.³⁵ The reactivity of WO_3 can however be low due to the lattice structure with large distances between Lewis acid and base sites.³⁶

ATR-IR revealed an increase in the thickness of hydrated WO_3 on the WC NP surface over time as deduced from the peaks at 895 and 960 cm^{-1} .³⁷ An example of this increase is shown for SW + 0.1 mM 3,4-DHBA in the inset of Fig. 4. Consistent with the lack of surface interactions between DHBA and the WC NPs, the presence of DHBA did not cause any significant changes in the zeta potential (values were approx. -20 mV). These observations are hence in line with the results in Fig. 2, showing no improvement in particle stability upon interaction with either DHBA or humic acid. For comparison, both DHBA molecules and humic acid adsorbed readily on Al NPs, Cu NPs, and Mn NPs through hydroxyl and carboxylate groups, as deduced by ATR-IR, a process that changed the zeta potential of these NPs (data not shown).

Conversely, soil with high natural organic matter contents (NOM \approx 90%) has shown a significantly higher capacity to adsorb tungsten compared with soil of lower NOM contents, which indicates an interaction with NOM.¹ WC NPs have also been shown to be stabilized by bovine serum albumin.³⁸ Clearly, more studies are needed to elucidate the interaction between tungsten alloys, including WC NPs, and NOM.

The dissolution of the WC NPs over time (defined as the total amount of tungsten able to pass through a 20 nm pore size membrane filter) and their corresponding release rates are shown in Fig. 5. The release kinetics changed with time with significantly higher initial release rates (<24 h) compared with those of the longer time periods. This behavior is different from the results of Andersson *et al.*³⁹ who showed linear release kinetics for WC particles. The observed long-term release rate (24–528 h) of tungsten was however similar with a value of approx. $1.6 \times 10^{-7} \text{ mole m}^{-2} \text{ h}^{-1}$,³⁹ compared with $1.4 \pm 0.4 \times 10^{-7} \text{ mole m}^{-2} \text{ h}^{-1}$ (in this study). Compared with other NPs, the dissolution rate of the WC NPs is in the same order as those reported for TiO_2 and Al_2O_3 NPs (first order $k_{\text{dissolution}}$ of approx. 10^{-8} s^{-1}).³³ The only significant differences in the release rates were observed for the WC NPs in SW + 3,4-DHBA compared with those for 2,3-DHBA and SW for 528 h, as deduced with a Student's *t*-test ($p < 0.05$). The



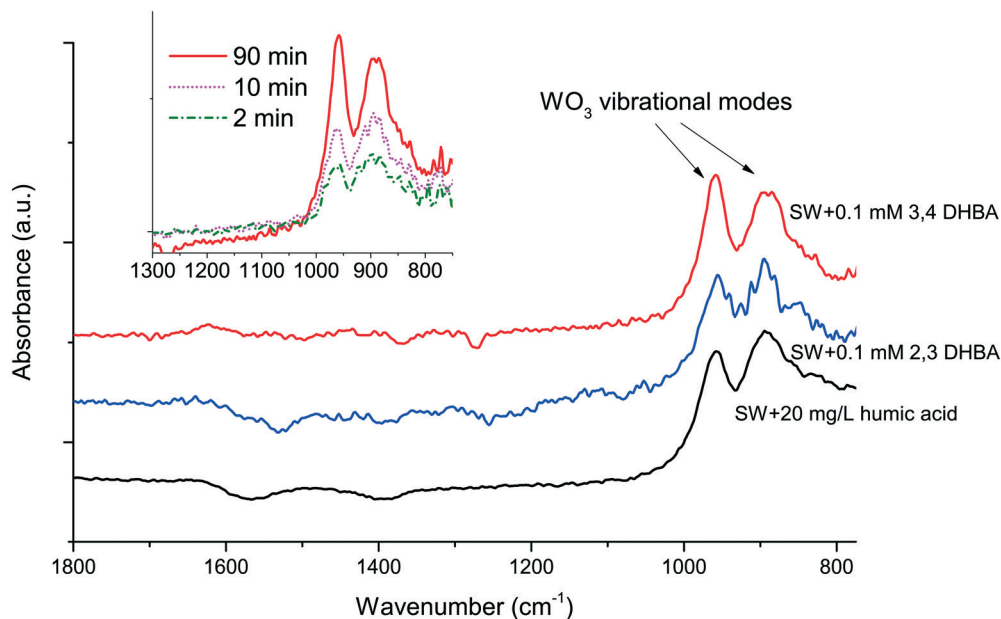


Fig. 4 ATR-IR spectra for WC NPs exposed to SW + 0.1 mM 2,3-DHBA, SW + 0.1 mM 3,4-DHBA, and SW + 20 mg L⁻¹ humic acid, at pH 6.2. All spectra were collected after 90 minutes of exposure, unless noted. The inset shows the time evolution of SW + 0.1 mM 3,4-DHBA for the WO₃ peaks. The spectra have been offset for clarity.

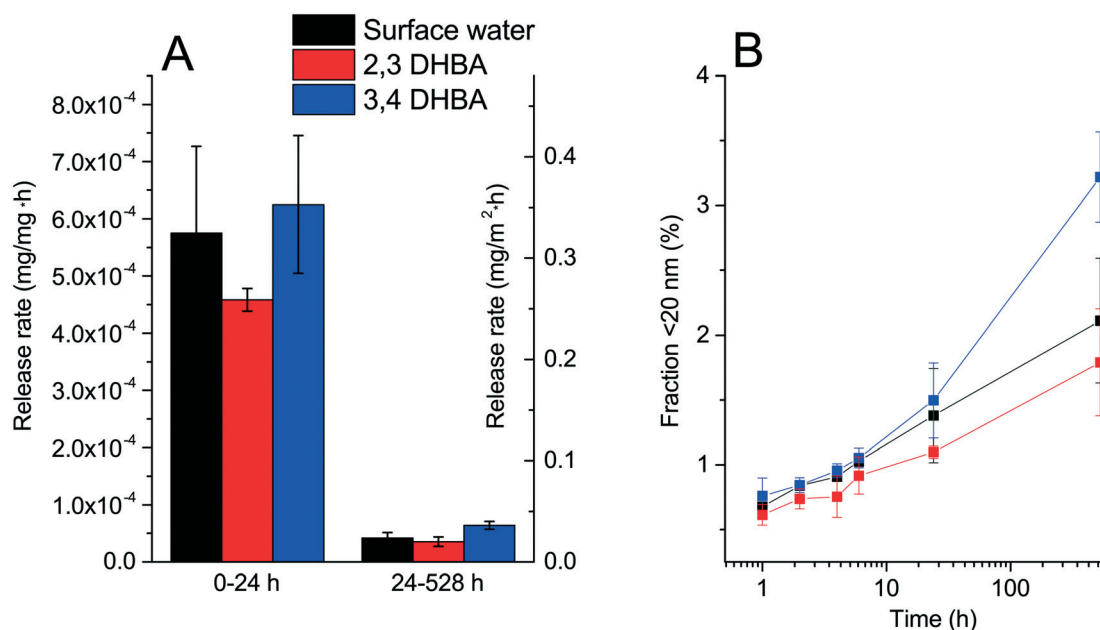


Fig. 5 A: Release rates of tungsten from WC NPs in surface water with and without DHBA molecules (0.1 mM). The release rates are based on the total amount of total W in the solution that is able to pass through a 20 nm pore size membrane filter. B: Kinetics of release of tungsten from WC NPs (note log-scale on the x-axis). All measurements were performed at pH 6.2. The error bars represent one standard deviation, derived from three independent measurements.

difference in the 528 h time point cannot be explained at this time. As no surface interactions were observed between DHBA and the WC NPs, the minor, or lack of, differences in the release rates between the different solutions are expected.

The speciation of released W from the WC NPs in SW and DHBA was estimated by JESS. The results showed that 100% of the soluble W exists as WO₄²⁻, both in SW and in SW + 2,3-DHBA and SW + 3,4-DHBA. It can however be noted that

the database used for the speciation of W did not contain any information on the binding constants between DHBA and W.

Upon further considering the possible negative effects of soluble tungsten, it can be noted that high concentrations, around a 1% mass basis, are needed for adverse effects in soil.¹² The particle size is important since the lower the tungsten particle radius, the lower the threshold for imparting toxicity to soil microbials.¹²



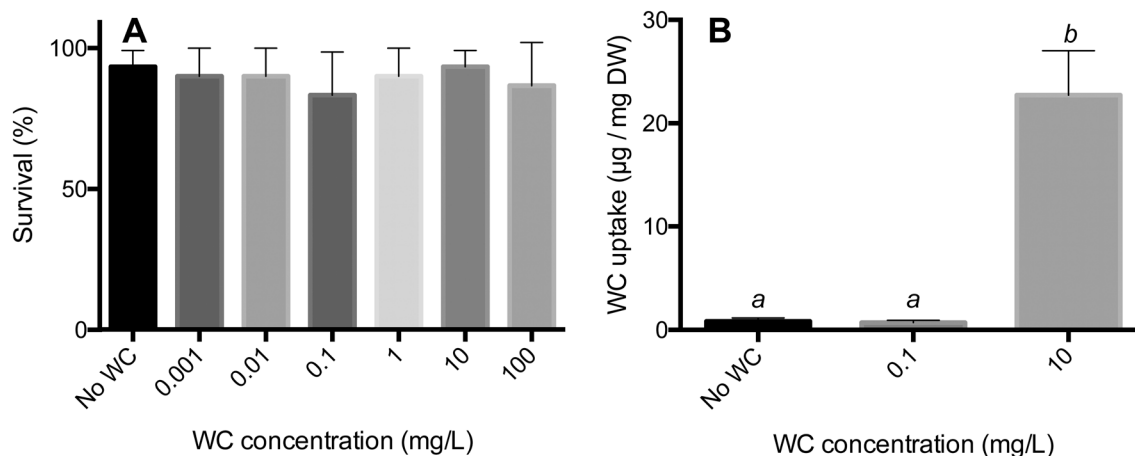


Fig. 6 A: Acute toxicity for *Daphnia magna* after 24 h of feeding on algae (*Scenedesmus* sp.) exposed to WC NPs for 24 h. B: Uptake of WC NPs by *Daphnia magna* after 24 h of feeding on algae (*Scenedesmus* sp.) exposed to WC NPs for 24 h. The different italic letters indicate significant differences (one-way ANOVA: $F_{2,42} = 26.21$, $P < 0.0001$).

Daphnia magna toxicity and uptake

The WC NPs did not cause any acute toxicity during a 24 h exposure for loadings between 100 and 0.001 mg mL⁻¹ (one-way ANOVA: $F_{6,14} = 0.3200$, $P = 0.9157$, Fig. 6A). Some mortality was observed in all treatments, and the highest recorded mortality in the control and WC NP treatments was 10% and 30%, respectively (Fig. 6A). However, all treatments had one replicate with a 100% survival, indicating that this mortality is likely caused by natural causes rather than the addition of WC NPs. One set of replicates was rerun as the mortality in the control for this set was above 20%. The highest concentration of WC NPs investigated herein (100 mg L⁻¹) is higher than the total concentration of tungsten found in the environment (e.g. up to 25 mg L⁻¹ in road runoff⁴⁰). The lack of acute toxicity by the WC NPs indicates no elevated toxicity compared to the soluble form of tungsten, as an EC₅₀ value of 89 mg L⁻¹ for W⁶⁺ has been determined for *D. magna*.¹³ As a comparison, the LC₅₀ values for Ag NPs have been reported to be in the range of 1–10 µg L⁻¹ for *D. magna*.⁴¹ Even though there were no acute effects observed, it is still unclear however if chronic effects may take place.

There was a significant difference in the amount of WC NPs taken up by *D. magna* in the different treatments (one-way ANOVA: $F_{2,42} = 26.21$, $P < 0.0001$). A Tukey's multiple comparison test revealed that the uptake in the 10 mg L⁻¹ treatment was significantly different from both the control and the 0.1 mg L⁻¹ treatment ($P < 0.0001$). The uptake in the 0.1 mg L⁻¹ treatment did not differ from that in the control ($P > 0.05$), Fig. 6B. The rate of uptake for the 24 h exposure to WC NPs was around 1 mg g⁻¹ (dry weight) h⁻¹, which is in the same order as that observed for e.g. TiO₂ (ref. 17) and Ag NPs.¹⁸ Significant agglomeration and sedimentation of the WC NPs as observed in the environmental media (Fig. 1) were also observed in the *D. magna* exposures (data not shown). Apparently, this did not hinder the uptake of WC NPs from taking place.

Conclusions

In this work, we have for the first time studied the interaction between NOM and WC NPs and investigated whether WC NPs induce any acute toxicity for *Daphnia magna*. The dissolution of tungsten from the WC NPs was continuous and the relatively low dissolution rate (on the order of 0.03 mg m⁻² h⁻¹) implies that transport will not be severely limited from a dissolution perspective. The affinity between the WC NPs and humic acid or DHBA was very low, with no evident surface adsorption taking place. The lack of surface interactions and stabilizing effects by these organic molecules, in combination with a relatively high effective density of WC NP agglomerates in humic acid, resulted in the substantial agglomeration and sedimentation of the WC NPs. The WC particle fraction sized around 150 nm remained for a longer time in the solution compared with the larger sized agglomerates. The smaller-sized fraction should hence be considered in future studies as it is this fraction that is most likely mobile and can be transported to other aquatic settings. Despite substantial particle agglomeration and sedimentation, WC NPs were clearly taken up by *D. magna*. This uptake may result in the bioaccumulation of WC in higher trophic level. However, no acute toxic effects were observed, even at concentrations higher than those recorded in the environment.

Acknowledgements

This work is a part of the Mistra Environmental Nanosafety program, and the financial support from Mistra is greatly acknowledged. Sara Isaksson, from KTH, is acknowledged for metal release and size distribution measurements. Alexandre Barreiro Fidalgo, from KTH, is acknowledged for help with ICP measurements. Nanxuan Mei, from KTH, is acknowledged for help with ATR-IR. Dr. Justin Teeguarden, from the Pacific Northwest Laboratory, USA, is acknowledged for providing the Matlab routine for the ISDD computations.



References

- 1 A. Koutsospyros, W. Braida, C. Christodoulatos, D. Dermatas and N. Strigul, *J. Hazard. Mater.*, 2006, **136**, 1–19.
- 2 H. Zheng, H. Huang, W. Wang and C. Ma, *Electrochem. Commun.*, 2005, **7**, 1045–1049.
- 3 Y. Yan, B. Xia, X. Qi, H. Wang, R. Xu, J.-Y. Wang, H. Zhang and X. Wang, *Chem. Commun.*, 2013, **49**, 4884–4886.
- 4 R. Lemus and C. F. Venezia, *Crit. Rev. Toxicol.*, 2015, **45**, 388–411.
- 5 A. T. Garcia-Esparza, D. Cha, Y. Ou, J. Kubota, K. Domen and K. Takanabe, *ChemSusChem*, 2013, **6**, 168–181.
- 6 D. Dermatas, W. Braida, C. Christodoulatos, N. Strigul, N. Panikov, M. Los and S. Larson, *Environ. Forensics*, 2004, **5**, 5–13.
- 7 J. L. Clausen and N. Korte, *Sci. Total Environ.*, 2009, **407**, 2887–2893.
- 8 P. Peltola and E. Wikström, *Boreal Environ. Res.*, 2006, **11**, 161–168.
- 9 M. S. Bučko, O.-P. Mattila, A. Chrobak, G. Ziolkowski, B. Johanson, J. Čuda, J. Filip, R. Zbořil, L. J. Pesonen and M. Leppäranta, *Geophys. J. Int.*, 2013, **195**, 159–175.
- 10 P. S. Bäuerlein, E. Emke, P. Tromp, J. A. Hofman, A. Carboni, F. Schooneman, P. de Voogt and A. P. van Wezel, *Sci. Total Environ.*, 2017, **576**, 273–283.
- 11 P. Peltola and M. Åström, *Environ. Geochem. Health*, 2003, **25**, 397–419.
- 12 N. Strigul, A. Koutsospyros, P. Arienti, C. Christodoulatos, D. Dermatas and W. Braida, *Chemosphere*, 2005, **61**, 248–258.
- 13 B. Khangarot and P. Ray, *Ecotoxicol. Environ. Saf.*, 1989, **18**, 109–120.
- 14 N. Strigul, A. Koutsospyros and C. Christodoulatos, *Ecotoxicol. Environ. Saf.*, 2010, **73**, 164–171.
- 15 G. R. Aiken, H. Hsu-Kim and J. N. Ryan, *Environ. Sci. Technol.*, 2011, **45**, 3196–3201.
- 16 N. Strigul, A. Koutsospyros and C. Christodoulatos, *Land Contam. Reclam.*, 2009, **17**, 189.
- 17 W. Fan, L. Liu, R. Peng and W.-X. Wang, *Sci. Total Environ.*, 2016, **569**, 1224–1231.
- 18 C.-M. Zhao and W.-X. Wang, *Environ. Sci. Technol.*, 2012, **46**, 11345–11351.
- 19 B. W. Strobel, *Geoderma*, 2001, **99**, 169–198.
- 20 C. J. Volk, *Methods in Enzymology, Microbial growth in biofilms*, Academic Press, New York, NY., 2001.
- 21 J. S. Taurozzi, V. A. Hackley and M. R. Wiesner, *Nanotoxicology*, 2011, **5**, 711–729.
- 22 S. Pradhan, J. Hedberg, E. Blomberg, S. Wold and I. Odnevall Wallinder, *J. Nanopart. Res.*, 2016, **18**, 285.
- 23 S. Brunauer, P. H. Emmet and E. Teller, *J. Am. Chem. Soc.*, 1938, **60**, 309–319.
- 24 J. M. Cohen, G. M. DeLoid and P. Demokritou, *Nanomedicine*, 2015, **10**, 3015–3032.
- 25 M. C. Sterling, J. S. Bonner, A. N. Ernest, C. A. Page and R. L. Autenrieth, *Water Res.*, 2005, **39**, 1818–1830.
- 26 P. M. Hinderliter, K. R. Minard, G. Orr, W. B. Chrisler, B. D. Thrall, J. G. Pounds and J. G. Teeguarden, *Part. Fibre Toxicol.*, 2010, **7**, 1.
- 27 H. J. Dumont, I. Van de Velde and S. Dumont, *Oecologia*, 1975, **19**, 75–97.
- 28 H. H. Bottrell, A. Duncan, M. Gliwicz, E. Grygierk, A. Herzig, A. Hillbricht-Ilkowska, H. Kurasawa, P. Larsson and T. Weglenska, *Norw. J. Zool.*, 1976, **24**, 419–456.
- 29 P. M. May, *Appl. Geochem.*, 2015, **55**, 3–16.
- 30 Y. Hedberg, J. Hedberg, S. Isaksson, N. Mei, E. Blomberg, S. Wold and I. Odnevall Wallinder, *Environ. Pollut.*, 2017, DOI: 10.1016/j.envpol.2017.02.006.
- 31 J. Cohen, G. DeLoid, G. Pyrgiotakis and P. Demokritou, *Nanotoxicology*, 2013, **7**, 417–431.
- 32 X.-Y. Li and B. E. Logan, *Water Res.*, 2001, **35**, 3373–3380.
- 33 J. T. Quik, J. A. Vonk, S. F. Hansen, A. Baun and D. Van De Meent, *Environ. Int.*, 2011, **37**, 1068–1077.
- 34 A. Praetorius, M. Scheringer and K. Hungerbühler, *Environ. Sci. Technol.*, 2012, **46**, 6705–6713.
- 35 A. Tocchetto and A. Glisenti, *Langmuir*, 2000, **16**, 6173–6182.
- 36 S. Ma and B. Frederick, *J. Phys. Chem. B*, 2003, **107**, 11960–11969.
- 37 M. Daniel, B. Desbat, J. Lassegues and R. Garie, *J. Solid State Chem.*, 1988, **73**, 127–139.
- 38 S. Bastian, W. Busch, D. Kühnel, A. Springer, T. Meißner, R. Holke, S. Scholz, M. Iwe, W. Pompe and M. Gelinsky, *Environ. Health Perspect.*, 2009, **117**, 530.
- 39 K. M. Andersson and L. Bergström, *Int. J. Refract. Hard Met.*, 2000, **18**, 121–129.
- 40 D. R. Bourcier, E. Hindin and J. C. Cook, *Int. J. Environ. Stud.*, 1980, **15**, 145–149.
- 41 S. Chernousova and M. Eppele, *Angew. Chem., Int. Ed.*, 2013, **52**, 1636–1653.

